Journal of Computational and Applied Mathematics 422 (2023) 114893

Contents lists available at ScienceDirect

Journal of Computational and Applied Mathematics

journal homepage: www.elsevier.com/locate/cam

Transient numerical approximation of hyperbolic diffusions and beyond

G. Leonenko [a], T.N. Phillips [b,*]

[a] School of Medicine, Cardiff University, Cardiff, United Kingdom
[b] School of Mathematics, Cardiff University, Cardiff, United Kingdom

ARTICLE INFO

Article history:
Received 8 February 2022
Received in revised form 21 September 2022

Keywords:
Hyperbolic diffusions
Fokker–Planck equation
Proper generalized decomposition
Spectral approximation

ABSTRACT

In this paper different types of hyperbolic diffusions and their corresponding transient Fokker–Planck equation are described and numerical solutions are presented. Diffusion models were developed that can fit both the marginal distribution and correlation structure and they have found a wide application in finance, turbulence and environmental time series. Hyperbolic diffusions have a complicated structure and variety of parameters and are extremely difficult to study and to model. We propose a numerical technique that solves the one-dimensional hyperbolic Fokker–Planck equation in the time dependent case. Note that this is the first study where transient hyperbolic diffusions are considered. The numerical technique is based on an adaptive reduced basis method using a spectral element discretization. It involves enrichment and projection stages where an optimal basis is found in a dynamic way using the singular value decomposition (SVD). The approach dramatically reduces the number of degrees of freedom required to solve the problem. The numerical simulations of the Fokker–Planck equation are verified with available stationary solutions.

1. Introduction

The hyperbolic distribution (HD) is a continuous probability distribution characterized by a probability density function for which the logarithm is a hyperbola, i.e. the log-density is hyperbolic. Recall that for normal distributions the log-density is parabolic. Thus the HD decreases more slowly than the normal distribution and therefore is more suitable for modelling certain classes of data. The use of distributions with semi-heavy or heavy tails leads to more realistic models than normal distributions when modelling phenomena where numerically large values are more probable.

The class of HDs is often used to fit the distributions of financial and environmental data and have been used in applications such as modelling turbulent wind speeds and in many other areas of science (see [1–4], for example). They have also been used in other fields. For example, in finance they have been used for valuation theories for derivative securities in which the distribution form of returns on the underlying assets plays a key role. Among the many models which have been investigated besides normal, stable Pareto and finite discrete combinations of normal distributions, it is the class of HDs which transpires to be an excellent candidate since it provides a more realistic model. In fact many data describing physical processes provide an excellent match to HD criteria. However, the complexity of the distribution and the lack of transient closed-form solutions have prevented researchers from using it to the full potential.

* Corresponding author.
E-mail address: PhillipsTN@cf.ac.uk (T.N. Phillips).

https://doi.org/10.1016/j.cam.2022.114893

From the historical point of view, HDs were formalized mathematically by Barndorff-Nielsen and co-workers [5,6], where the generalized hyperbolic distribution (GHD) was also introduced, using the fact that the HD is a random combination of normal distributions. In these papers the distributions were applied to the study of grains of sand.

There are fundamental connections between the theory of diffusion and the theory of probability. In mechanics, the diffusion or Fokker–Planck (FP) equation is a partial differential equation that describes the time evolution of the probability density function (pdf) of the velocity of a particle under the influence of drag and random Brownian forces. The equation is also known as the Kolmogorov forward equation in the theory of stochastic differential equations driven by Brownian motion. It is well known that the Fokker–Planck equation with constant coefficients driven by Brownian motion is also known as the Ornstein–Uhlenbeck process. The solutions resulting from the process are useful to model diffusive phenomena in which particles move in a homogeneous environment.

In a heterogeneous environment, the coefficients of the Fokker–Planck or diffusion equation will naturally vary in space. We consider here a tractable class of variable coefficient diffusion models that govern a class of Markov processes whose steady-state distributions belong to the class of HDs. For diffusions with spatially varying coefficients, analytical expressions for the transient solution of the Fokker–Planck equation or the transition densities of governing Markov processes are not available and therefore numerical methods must be developed and explored. To the best of our knowledge this paper represents the first study of transient solutions of hyperbolic diffusions which is of intrinsic interest.

In this paper we use a numerical method for the solution of transient Fokker–Planck equations with spatially variable coefficients. The method is based on the high-order reduced basis approximation proposed in the papers by Leonenko and Phillips [7–9]. The underlying spatial discretization is based on a spectral approximation. In spectral methods the solution of a differential equation is approximated using the eigenfunctions of a singular Sturm–Liouville problem as basis functions. These eigenfunctions are used since the rate of decay of the expansion coefficients is determined solely by the smoothness of the solution and not by any special conditions satisfied by the solution at the boundary. Typically either Chebyshev or Legendre polynomials are used. Unlike the finite element method, spectral methods generate discrete equations that involve relationships between the unknowns that are not necessarily local. The approximations generated in this way are extremely accurate when the solution is smooth and require considerably fewer degrees of freedom to achieve a given level of accuracy compared with local discretization methods such as finite differences and finite elements. They have been used widely to solve problems in fluid mechanics — see the monograph of Canuto et al. [10], for example. In this paper we use spectral approximations based on Legendre polynomials and the discrete weak formulation of the problem is derived using Gaussian quadrature based on the Gauss–Lobatto Legendre points.

Model reduction techniques have gained considerable popularity and success over the last decade or so (see the papers of Chinesta and co-workers [11–14] and the book of Chinesta et al. [15]). Model reduction works particularly well if one has knowledge of the approximate solution of a given problem a priori. In this case one can build a reduced-order approximation. However, it is far more useful to be able to construct reduced-order models without knowledge of the solution, be it approximate or exact. The Proper Generalized Decomposition (PGD) achieves this in an efficient manner. The method is based on a dynamic construction of a separated variable basis in which the basis is continuously enriched until a given level of accuracy is achieved. This method was successfully applied to the class of so-called Pearson diffusions with linear drift and quadratic squared diffusion term and their related transient Fokker–Planck equation by Leonenko and Phillips [8]. Furthermore, high-dimensional Fokker–Planck equations and their related multi-dimensional diffusions with polynomial coefficients have also been solved numerically [9].

Note, that we also use approximations of diffusion-type models found in the paper of Bibby et al. [16] that are based on the saddle point technique. It is used in cases where no tractable analytical expressions for the diffusion coefficient are available and therefore efficient and accurate numerical approximations are vital.

The paper is organized in the following way. In Section 2 the hyperbolic diffusions are defined and their different classes and relationships are described. The associated hyperbolic stochastic differential equations are presented along with some of their properties. In Section 3 the numerical approximation of the transient Fokker–Planck using a high-order reduced basis approximation is described. Section 4 illustrates the application of the numerical algorithm to important classes of hyperbolic diffusions. Although the accuracy of the transient solution cannot be assessed since analytical closed form expressions do not exist, the accuracy of the steady state numerical approximation with the distribution itself is studied and quantified. These numerical examples illustrate the excellent approximation properties of the high-order numerical solutions developed in this paper.

2. Hyperbolic diffusions

Consider the diffusion process $X(t), t \geq 0$, that is governed by the Fokker–Planck equation

$$\frac{\partial}{\partial t}p(x,t) = -\frac{\partial}{\partial x}[\mu(x)p(x,t)] + \frac{1}{2}\frac{\partial^2}{\partial x^2}[\sigma^2(x)p(x,t)], \quad x \in \mathbb{R}, \quad t \geq 0, \tag{1}$$

with point source initial condition

$$p(x,0) = p(x,0;y) = \delta(x-y),$$

where $p(x,t) = p(x,t;y),\ t > 0,\ x,\ y \in \mathbb{R}$, denotes the conditional probability density of $x = X(t)$ given $y = X(0)$, i.e. the transition probability density of the time-homogeneous Markov process $X(t), t \geq 0$, which satisfies the stochastic differential equation (SDE) in the Itô sense:

$$dX(t) = \mu(X(t))dt + \sigma(X(t))dW(t),\quad t \geq 0, \tag{2}$$

where $W(t),\ t \geq 0$, is a standard Brownian motion and the functions $\mu(\cdot)$ and $\sigma^2(\cdot) \geq 0$ are, respectively, the drift and diffusion coefficients of the process. If the time-homogeneous Markov process $X(t), t \geq 0$, is steady-state, then its probability density $f(x)$ stays the same over all times. In this paper we assume that the steady-state or ergodic distribution $f(x)$ belongs to the class of HDs, that is $\log(f(x))$ is a hyperbola. Note that for a constant coefficient diffusion, that is for the case when $\mu(x) = \mu \in \mathbb{R}, \sigma(x) = \sigma > 0$, the steady-state distribution of a Markov process $X(t),\ t \geq 0$, known as the Ornstein–Uhlenbeck process, is normal or Gaussian, which means that $\log(f(x))$ is a parabola. All SDEs considered here possess a weak solution.

In this section we review the key definitions and properties related to the general class of hyperbolic diffusions and classify them into two broad classes of distribution: generalized hyperbolic distributions (GHD) and generalized inverse Gaussian distributions (GIG). We also make use of basic facts about diffusion models, whose steady-state distributions belong to the class of HDs.

The structure of the diffusion term in Eq. (1) is complicated and it is not possible to find theoretical expressions for transient solutions. Therefore in our study we focus on obtaining numerical approximations for their transient solutions $p(x,t), x \in \mathbb{R}, t \geq 0$, using ideas developed in the papers of Ammar et al. [17] and Leonenko and Phillips [7–9] using reduced basis methods and high-order spectral approximations.

2.1. Generalized hyperbolic distributions (GHD)

The first class of distributions to be considered is the GHD which was introduced and studied by Barndorff-Nielsen [5] (see also [1,6,16]). This class includes the normal inverse Gaussian (NIG), scaled t-distributions, and variance gamma (VG).

We begin by summarizing key information about GHDs. GHDs are characterized by five parameters

$$X \sim H(\lambda, \alpha, \beta, \delta, \mu), \tag{3}$$

and has probability density function given by

$$gh(x) = \frac{(\gamma/\delta)^\lambda}{\sqrt{2\pi}K_\lambda(\delta\gamma)} \frac{K_{\lambda-\frac{1}{2}}\left(\alpha\sqrt{\delta^2+(x-\mu)^2}\right)}{\left(\sqrt{\delta^2+(x-\mu)^2}/\alpha\right)^{\frac{1}{2}-\lambda}} e^{\beta(x-\mu)},\ x \in \mathbb{R}, \tag{4}$$

where $\gamma^2 = \alpha^2 - \beta^2$ and

$$K_\lambda(x) = \frac{1}{2}\int_0^\infty u^{\lambda-1}e^{-\frac{1}{2}x(u+u^{-1})}du,\ x > 0,$$

is the modified Bessel function of the third kind with index λ.

The parameter domain for the generalized hyperbolic function is given by

$$\begin{array}{lllll} \delta \geq 0, & a > 0, & \alpha^2 > \beta^2, & \text{if } \lambda > 0, \\ \delta > 0 & a > 0 & \alpha^2 > \beta^2 & \text{if } \lambda = 0, \\ \delta > 0 & a \geq 0 & \alpha^2 \geq \beta^2 & \text{if } \lambda < 0. \end{array} \tag{5}$$

In all cases $\mu \in \mathbb{R}$. Note that if $\beta = 0$, the distribution is symmetric. The class of GHDs is closed under affine transformation. Expressions for the Laplace transform, expectation and variance can be found in Barndorff-Nielsen [5] and Bibby et al. [16].

The special classes of the GHD:

1. Variance Gamma Diffusion. This distribution is obtained when $\delta = 0$ and is only possible when $\lambda > 0$ and $\alpha > |\beta| \geq 0$ and $\mu \in \mathbb{R}$. This distribution is considered in Section 4.2 of the current paper.
2. Student Diffusion. This distribution is obtained when $\alpha = \beta = 0$ and is only possible when $\lambda < 0$ and $\delta > 0$. This diffusion and also the skew Student diffusion belong to the Pearson class of diffusions and have been investigated by Leonenko and Phillips [8].

2.2. Generalized inverse Gaussian (GIG) distributions

The second class is a class of generalized inverse Gaussian distributions (GIG). The GIG-distributions are described by three parameters and defined on the positive real axis. The probability density function of the generalized inverse Gaussian is of the form

$$gig(x) = \frac{(\gamma/\delta)^\lambda}{2K_\lambda(\delta\gamma)} x^{\lambda-1}\exp\left\{-\frac{1}{2}(\delta^2 x^{-1} + \gamma^2 x)\right\},\ x > 0. \tag{6}$$

The parameter domain is given by

$$\begin{array}{llll} \delta > 0, & \gamma \geq 0, & \text{if} & \lambda < 0, \\ \delta > 0, & \gamma > 0 & \text{if} & \lambda = 0, \\ \delta \geq 0, & \gamma > 0 & \text{if} & \lambda > 0. \end{array} \tag{7}$$

This class of distributions was first applied to model the distribution of the monthly flow of water in hydroelectric stations and then rediscovered in finance. It is interesting to note that GIG is an intermediate distribution lying somewhere between Pearsons' class of Type III and V [18].

The special classes of the GIG distributions are:

1. Inverse Gamma Diffusion. This distribution is obtained when $\gamma > 0$, $\lambda < 0$, and $\delta > 0$. This distribution has been investigated in Leonenko and Phillips [8].
2. Inverse Gaussian distribution. This distribution is obtained when $\lambda > -1/2$, $\gamma > 0$ and $\delta > 0$. This distribution is considered in Section 4.1 in this paper.

There exists the following important relationship between the GHD and GIG distributions, which was, in fact, how the generalized hyperbolic distribution was originally derived by Barndorff-Nielsen [5]. The GHD is a normal variance-mean mixture where the mixing distribution is GIG.

2.3. Hyperbolic stochastic differential equations

We begin by describing the construction of diffusion processes by means of stochastic differential equations (SDEs) with an exponential autocorrelation function and specified marginal distributions on the interval (l, r), $-\infty \leq l < r \leq \infty$, which have a pre-specified density $f(x)$ with respect to the Lebesgue measure on the state space (l, r) (see Bibby et al. [16]).

This means that we study stochastic processes $X = \{X(t), t \geq 0\}$ which satisfy the Itô SDE:

$$dX(t) = \mu\left(X(t)\right) dt + \sqrt{\upsilon(X(t))} dW(t), \quad t \geq 0, \tag{8}$$

where $W = \{W(t), t \geq 0\}$ is a standard Brownian motion and the functions $\mu(\cdot)$ and $\upsilon(\cdot) = \sigma^2(\cdot) \geq 0$ are, respectively, the drift and diffusion coefficients of the process.

In this paper the following classes of SDE are considered:

$$dX(t) = -\theta(X(t) - \mu)dt + \sqrt{\upsilon(X(t))} dW(t), \quad t \geq 0, \tag{9}$$

where $\theta > 0$, $\mu \in (l, r)$.

Given a hyperbolic steady-state distribution $f(x)$ one can compute the corresponding diffusion function as follows

$$\upsilon(x) = \frac{2\theta}{f(x)} \int_l^x (\mu - u) f(u) du, \quad l < x < r, \tag{10}$$

where we assume

$$\int_l^r \upsilon(x) f(x) dx < \infty \tag{11}$$

and the probability density function f is continuous, bounded, strictly positive and has compact support on (l, r).

From Bibby et al. [16] it follows:

(a) The SDE (9) has a unique Markov weak solution and the diffusion coefficient $\upsilon(\cdot)$ given by (10) is strictly positive on (l, r).
(b) The diffusion process X that solves the SDE (9) is ergodic with invariant density f.
(c) The condition (11) is satisfied. If X is stationary the autocorrelation function for X has the form:

$$\mathrm{E}\left(X(s+t)|X(s) = x\right) = xe^{-\theta t} + \mu\left(1 - e^{-\theta t}\right),$$

(d) If $-\infty < l$ or $r < \infty$, then the diffusion given by (9) is the only ergodic diffusion with drift and invariant density f for which (11) is satisfied.

All the special classes of GHD and GIG distributions that are considered in this paper are mean-reverting. Additionally, we consider the F-distribution process that belongs to the class of mean-reverting diffusions but does not belong to the GHD or GIG distributions (see Section 4.4). This class belongs to the heavy-tailed diffusions.

We consider the Cubic process that does not belong to class of GHD and GIG distributions, see Gutierrez at al. [3] which satisfies the SDE (8)) of the form

$$dX(t) = \mu(X(t))dt + \sigma(X(t))dW(t), \quad t \geq 0, \tag{12}$$

where $\mu(x) = Ax^3 + Bx$, $\sigma^2(x) = C^2x^4$.

3. Formulation of the problem and spectral discretization

Consider the numerical approximation of the Fokker–Planck equation (1), and corresponding Markov process which satisfies SDE (12). This Fokker–Planck equation is valid for the conditional density, $p(x, t), t \geq 0, x \in \mathbb{R}$ of the variable $X(t) = \{x|X(t_0) = x_0\}$ of the corresponding homogeneous Markov process with the state space, Ω, that is, for any initial x_0, t_0.

In this paper, a modification of the scheme that was used by Leonenko and Phillips [7–9] to predict the evolution of the configuration density associated with kinetic theory models in polymer dynamics is described. The method is based on an adaptive reduced basis approximation to the Fokker–Planck equation. The method was first proposed by Ammar et al. [17] in the context of the finite element method. The idea underlying basis reduction comes from finding an approximate singular value decomposition (SVD) and it provides us with an efficient method for constructing basis functions in a dynamic fashion that contains the most representative information about the solution. Leonenko and Phillips [7–9] have extended this procedure to develop spectral approximations to the solution of the high-dimensional Fokker–Planck equation derived from the equation of motion for the beads in an elastic dumbbell model for dilute polymer solutions. In this paper we use an implicit scheme to solve the one-dimensional problems arising in the study of hyperbolic diffusion processes.

The simplest implicit temporal scheme, the backward Euler method, was used in this study. An alternative is the Crank–Nicolson method which is second-order accurate but at the expense of requiring additional evaluations of the drift and diffusion terms. The backward Euler discretization of Eq. (1) is

$$\frac{p(x, t^{n+1}) - p(x, t^n)}{\Delta t} = -\frac{\partial}{\partial x}[\mu(x)p(x, t^{n+1})] + \frac{1}{2}\frac{\partial^2}{\partial x^2}[\sigma^2(x)p(x, t^{n+1})], \tag{13}$$

where Δt is the time step and $t^n = n\Delta t$. We have assumed that the drift and diffusion coefficients are independent of time. If p^* is a suitable test function that satisfies homogeneous initial and boundary conditions, then we can formulate a weak formulation of this semi-discrete problem by multiplying Eq. (13) by p^* and integrating over the interval $I = [c, d]$:

$$\int_I p^* \left(\frac{p(x, t^{n+1}) - p^n(x, t^n)}{\Delta t}\right) dx + \int_I p^* \frac{\partial}{\partial x}[\mu(x)p(x, t^{n+1})]\, dx - \frac{1}{2}\int_I p^* \frac{\partial^2}{\partial x^2}\left[\sigma^2(x)p(x, t^{n+1})\right] dx = 0. \tag{14}$$

3.1. Representation of the solution and spectral discretization

The solution of Eq. (14) is assumed to have the following form:

$$p(x, t^{n+1}) = \sum_{j=1}^{\infty} \alpha_j^{n+1} g_j^{n+1}(x), \tag{15}$$

where the coefficients α_j^{n+1} and basis functions $g_j^{n+1}(x)$ are time-dependent. To simplify the notation we drop the superscript $n + 1$ on terms on the right-hand side of Eq. (15). Note that the test function can be represented as follows:

$$p^*(x, t^{n+1}) = \sum_{j=1}^{\infty} \alpha_j^* g_j(x). \tag{16}$$

The basis functions $g_j(x)$ are represented using Lagrangian interpolating polynomials associated with the Gauss–Lobatto Legendre nodes, i.e. the zeros of $(1 - x^2)L'_N(x)$, where $L_N(x)$ is the Legendre polynomial of degree N. More specifically, we have

$$g_j(x) = \sum_{k=0}^{N} g_{j,k} h_k(x) \tag{17}$$

and $g_{j,k} = g_j(x_k)$, $k = 0, \ldots, N$, are unknown coefficients. In the case of an approximation of degree N, the Lagrangian interpolants, h_k, are defined by

$$h_k(x) = \frac{(1 - x^2)L'_N(x)}{N(N + 1)L_N(x_k)(x - x_k)}. \tag{18}$$

The entries of the Legendre differentiation matrix, $\hat{D}_N$, are given by

$$(\hat{D}_N)_{j,k} = h'_k(x_j) = \begin{cases} \frac{L_N(x_j)}{L_N(x_k)}\frac{1}{(x_j - x_k)}, & j \neq k, \\ -\frac{(N+1)N}{4}, & j = k = 0, \\ \frac{(N+1)N}{4}, & j = k = N, \\ 0 & \text{otherwise.} \end{cases} \tag{19}$$

Note that the integrals in Eq. (14) are approximated using the Gauss–Lobatto Legendre quadrature rule

$$\int_{-1}^{1} f(x)dx \approx \sum_{j=0}^{N} f(x_j)w_j, \tag{20}$$

where the weights are given by

$$w_j = \frac{2}{N(N+1)(L_N(x_j))^2}. \tag{21}$$

This quadrature rule is exact whenever f is a polynomial of degree $2N-1$ or less.

The procedure for determining the numerical approximation at each time step comprises two stages. The basis functions are determined dynamically using an enrichment procedure to augment the basis followed by the determination of the coefficients in the expansion using projection. The algorithm is initiated with the determination of the first basis function $g_1(x)$ using enrichment.

At the Jth stage of the algorithm, given the basis functions $g_j(x)$, $j = 1, \ldots, J$, the coefficients α_j, $j = 1, \ldots, J$, are computed using projection. This is followed by an enrichment of the basis in which $g_{J+1}(x)$ is determined. The reduced basis method proceeds in an iterative manner until convergence is obtained. More precisely, the algorithm at a given time step is terminated when $|\alpha_J| < 10^{-7}$.

The algorithm is terminated when steady state is reached at time $t = T$. A schematic flow diagram showing the principal steps of the algorithm is shown in Fig. 1.

The algorithm presented in this paper differs from previous applications of the classical PGD approach in several respects. The coefficients in the expansion of the solution given by Eq. (15) are time-dependent as are the basis functions g_j^n. In addition, the basis functions are determined dynamically at each time step and form an orthonormal basis. The dynamic nature of the basis functions means that the rank, J, of the basis can vary over time. This orthonormal property of the basis has computational advantages since it results in simpler linear systems. The use of a spectral rather than a finite element representation of the basis functions means that a low rank approximation is usually obtained. The use of a spectral approximation results in extremely rapid spatial convergence leading to great accuracy with few degrees of freedom.

3.2. Projection stage

The purpose of the projection stage is to compute the coefficients $j = 1, \ldots, J$, in the representation given by Eq. (15). In this stage, the basis functions $g_j(x)$, $j = 1, \ldots, J$, are known. Thus, inserting the approximations formed by truncating Eqs. (15) and (16) to J terms into the discrete weak formulation of the problem (14) and simplifying the result yields the following linear system:

$$M\boldsymbol{\alpha} = \mathbf{v}, \tag{22}$$

where $\boldsymbol{\alpha} = (\alpha_1, \ldots, \alpha_J)^T$ and M is the $J \times J$ matrix with entries defined by

$$M_{i,j} = \boldsymbol{g}_i^T(B + \Delta t A)\boldsymbol{g}_j \tag{23}$$

and the components of the right-hand side vector $\mathbf{v}$ are given by

$$v_i = \boldsymbol{g}_i^T B\boldsymbol{p}^n, \tag{24}$$

where $p_i^n = p(x_i, t^n)$.

The entries of the $N \times N$ matrices A and B are defined by

$$A_{m,n} = -w_n\mu(x_n)(\hat{D}_N)_{n,m} + \frac{1}{2}\sum_{l=0}^{N}\sigma^2(x_l)w_l(\hat{D}_N)_{l,m}(\hat{D}_N)_{l,n}, \tag{25}$$

$$B_{m,n} = w_m\delta_{m,n}. \tag{26}$$

Note that the basis functions $\{g_j\}$ are constructed to be orthonormal with respect to the discrete inner product, i.e. $\boldsymbol{g}_i B\boldsymbol{g}_j = \delta_{ij}$. Once $\boldsymbol{\alpha}$ has been determined by solving Eq. (22), we have the best rank J approximation to the solution and we proceed to the enrichment stage. In practice, we have found that $J \leq 3$ is usually sufficient to obtain a converged approximation, so the system (22) is very small and computationally inexpensive to solve.

3.3. Enrichment stage

In this stage, the basis is enriched by adding an additional function $r(x)$ to the basis. Assuming knowledge of $g_j(x)$, and α_j, $j = 1, \ldots, J$, we write the new approximation in the form:

$$p(x, t^{n+1}) = \sum_{j=1}^{J}\alpha_j g_j(x) + r(x), \tag{27}$$

where $r(x)$ is expressed in the form

$$r(x) = \sum_{k=0}^{N} r_k h_k(x). \tag{28}$$

The test functions used in the weak formulation are given by

$$p^*(x) = h_j(x),\ j = 0, \ldots, N.$$

This results in the following linear system for the unknown coefficients r_k, $k = 0, \ldots, N$, in the representation of the new basis function given by Eq. (28):

$$(B + \Delta t A)\mathbf{r} = \mathbf{c}, \tag{29}$$

where

$$\mathbf{c} = B\mathbf{p}^n - \sum_{j=1}^{J} \alpha_j (B + \Delta t A)\mathbf{g}_j.$$

To normalize the solution we evaluate

$$\mathbf{r}_{new} = \frac{\mathbf{r}}{\sqrt{\mathbf{r}^T B \mathbf{r}}}. \tag{30}$$

The solution of this linear system furnishes the coefficients r_k in the expansion of the new basis function $r(x)$. Finally, we set

$$g_{J+1}(x) = r(x). \tag{31}$$

Concerning the computational cost, this step consumes the main part of the global computing time. Note, however, that the solver normally converges very quickly and in the one-dimensional case only one enrichment step is usually required to accurately approximate the solution.

4. Numerical examples

The spatial approximation of the solution uses basis functions with $N = 80$. This is sufficient to obtain spatial convergence for all the examples considered in this section. The algorithm terminates at $t = 10$ and a time step $\Delta t = \frac{1}{3}$ was used. It is assumed that by this time the approximation has reached steady state.

In all the numerical examples that follow the mean absolute relative error at steady state is computed i.e.

$$E_{rel} = \frac{\sum_{k=0}^{N} |p_n(x_k) - p(x_k)|}{\sum_{k=0}^{N} |p(x_k)|}.$$

The value of E_{rel} is provided in the figure caption for each diffusion considered. Temporal convergence was checked by halving the time step and by doubling the time over which computations are performed to $t = 20$. In both cases the value of E_{rel} remained unchanged.

4.1. Inverse Gaussian diffusion

Consider the solution of the following Fokker–Planck equation

$$\frac{\partial}{\partial t} p(x, t) = -\frac{\partial}{\partial x}[-\theta(x - \mu)p(x, t)] + \frac{1}{2}\frac{\partial^2}{\partial x^2}[\upsilon(x)p(x, t)], \quad x \in \mathbb{R}, t \geq 0. \tag{32}$$

The *inverse Gaussian diffusion* process with ergodic density

$$ig(x) = \frac{\delta e^{\gamma/\delta}}{\sqrt{2\pi x^3}} e^{-\frac{1}{2}(\delta^2/x + \gamma^2 x)},\ \delta > 0,\ x > 0,$$

with

$$\mu = \delta/\gamma \quad \text{and} \quad \upsilon(x) = \frac{2\theta\delta}{\gamma \cdot ig(x)} e^{2\gamma\delta} \Phi\left(-\frac{(\gamma x + \delta)}{\sqrt{x}}\right),$$

where

$$\Phi(x) = \int_{-\infty}^{x} \frac{e^{-t^2/2}}{\sqrt{2\pi}} dt.$$

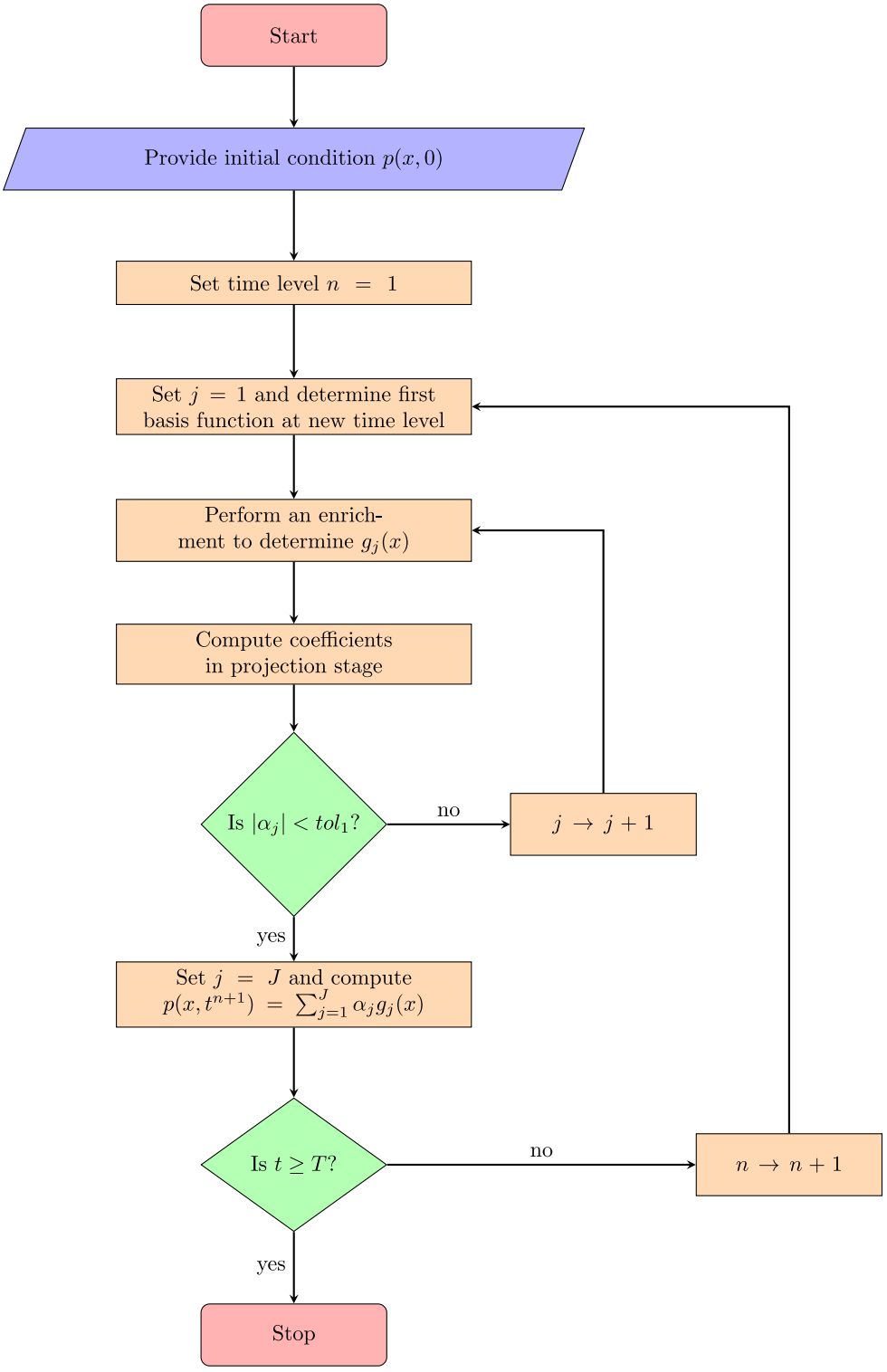

Fig. 1. Flow chart of algorithm where $tol_1 = 10^{-7}$.

The diffusion term can be approximated using (see Bibby et al. [16]).

$$\tilde{v}(x) = \frac{4\theta x^2}{\gamma^2(x + \delta/\gamma)}. \tag{33}$$

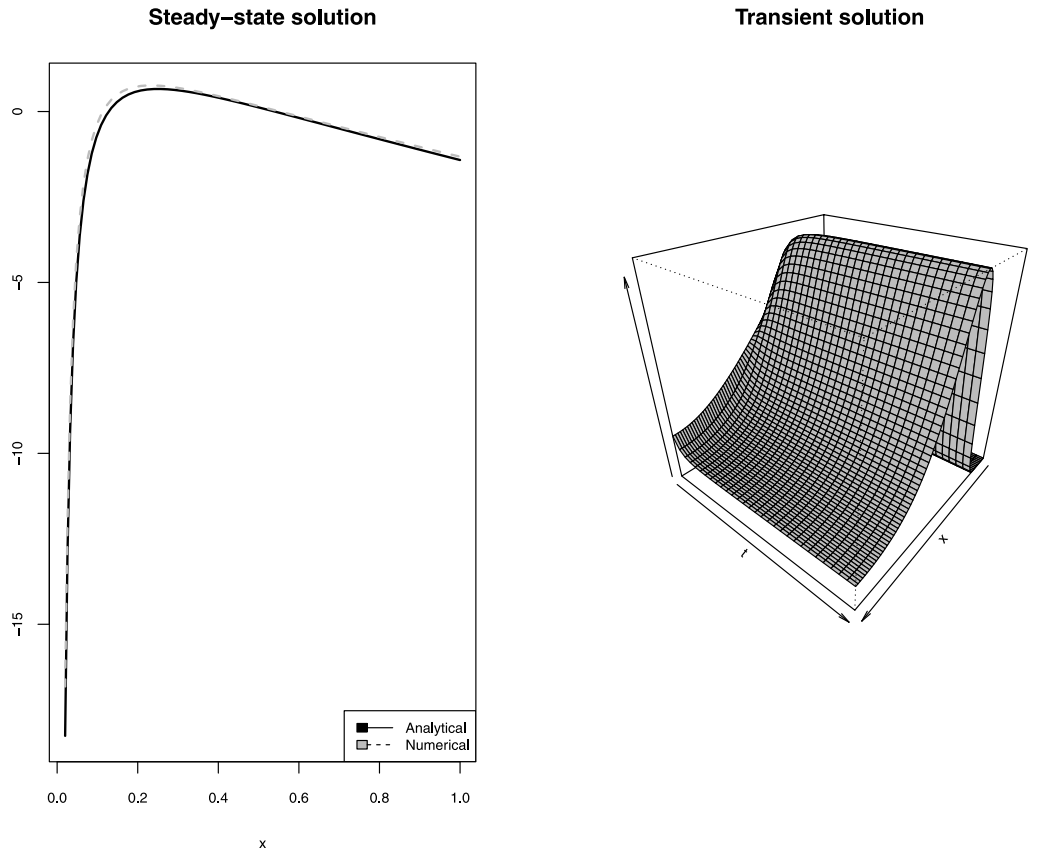

Fig. 2. Inverse Gaussian diffusion with $\theta = 1$, $\gamma = 2$, $\delta = 1$. (a) Comparison of the numerical and analytical steady-state solutions in log scale. (b) Transient numerical solution. $E_{rel} = 0.008$.

The same results are obtained using either the diffusion term or its approximation. Obviously, the form of the approximate diffusion term given in (33) is relatively simple and therefore very easy to implement computationally.

Fig. 2(a) presents the numerical approximation of inverse Gaussian diffusion on log scale when it converges to the steady-state solution with parameters $\theta = 1$, $\gamma = 4$, $\delta = 1$. For the reduced basis approximation we use two basis function and $\alpha_0 = 2.16432$ and $\alpha_1 = 4.07139 \times 10^{-15}$. Fig. 2(b) presents the transient behaviour of the numerical solution using the same parameters. For this problem we have mean absolute relative error $E_{rel} = 0.008$.

4.2. Variance Gamma diffusion

The Variance Gamma (VG) distribution is a special case of the GHD that has proved to be useful in the modelling of turbulence and financial data. The probability density function of this distribution is given by

$$ng(x) = \frac{(\alpha^2 - \beta^2)^{\lambda}}{\sqrt{\pi}\,\Gamma(\lambda)(2\alpha)^{\lambda-\frac{1}{2}}} |x-\delta|^{\lambda-\frac{1}{2}} K_{\lambda-\frac{1}{2}}(\alpha|x-\delta|) e^{\beta(x-\delta)}, \quad x \in \mathbb{R}, \tag{34}$$

where Γ denotes the Gamma function and K_λ is modified Bessel function of the third kind, and where $\lambda > 0$ and $\alpha > |\beta| \geq 0$ and $\delta \in \mathbb{R}$, see, i.e., [19].

The Fokker–Planck equation in this case has the form:

$$\frac{\partial}{\partial t} p(x,t) = -\frac{\partial}{\partial x}[-\theta(x-\mu)p(x,t)] + \frac{1}{2}\frac{\partial^2}{\partial x^2}[\upsilon(x)p(x,t)], \quad x \in \mathbb{R}. \tag{35}$$

$$\mu = \delta + \frac{2\beta\lambda}{\alpha^2 - \beta^2}$$

In the case when $\beta = 0$, the diffusion term can be determined explicitly

$$\upsilon(x) = |x-\mu| \frac{K_{\lambda+\frac{1}{2}}(\alpha|x-\mu|)}{K_{\lambda+\frac{1}{2}}(\alpha|x-\mu|)}.$$

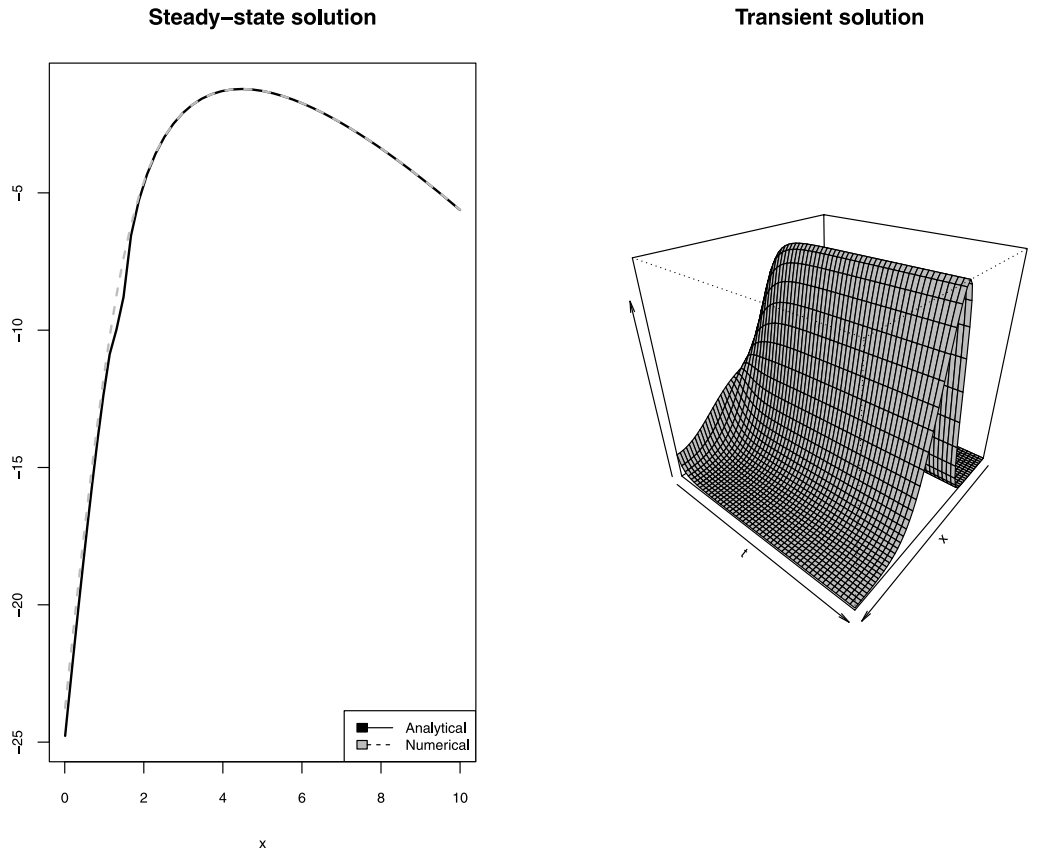

Fig. 3. Variance gamma diffusion with $\theta = 1$, $\alpha = 10$, $\beta = 8$, $\delta = 1.41$, $\lambda = 8$. (a) Comparison of the numerical and analytical steady-state solutions in log scale. (b) Transient numerical solution. $E_{rel} = 0.003$.

However in other cases it is not possible to determine an explicit expression for the squared diffusion coefficient. Nevertheless, in this case an approximation of the diffusion term can be used, such as the one proposed by Bibby and Sorensen [2]:

$$\tilde{\upsilon}(x) = \begin{cases} \frac{4\theta\lambda}{\alpha^2-\beta^2}, & x = \delta \\ \frac{2\theta(x-\delta)(x-\delta-2\beta\lambda/(\alpha^2-\beta^2))}{\sqrt{\lambda^2+\alpha^2(x-\delta)^2}-\lambda-\beta(x-\delta)}, & x \neq \delta. \end{cases} \tag{36}$$

The advantage of this approximation is that it provides good accuracy and more importantly has an explicit form.

Fig. 3(a) presents the numerical approximation of the variance gamma diffusion on log scale when it converges to the steady-state solution with parameters $\theta = 1, \lambda = 1, \alpha = 10, \beta = 8, \delta = 1.41$. For the reduced basis approximation we use two basis function and $\alpha_0 = 0.2043598$ and $\alpha_1 = 4.77743 \times 10^{-16}$. Fig. 3(b) presents the transient numerical solution with the same parameters.

4.3. Cubic drift diffusion

This interesting diffusion appeared in Gutierrez et al. [3] and has been used in applications such as the modelling and prediction of global CO_2 emissions. This process is original and novel and can be statistically fitted to real cases of growth within a stochastic environment. It can be used to fit environmental growth trends and to analyse possible anomalies affecting such trends. The behaviour of growth phenomena, in general, is affected by environmental fluctuations that are responsible for the discrepancies between experimental data and the corresponding theoretical predictions.

This diffusion with cubic drift for the phenomena described above can be written as

$$dX(t) = (AX(t)^3 + BX(t))dt + CX^2(t)dW(t),\ t \geq 0, \tag{37}$$

with initial condition $P[X_{t_0} = x_{t_0}] = 1$. It is easily proved that the drift and diffusion terms are Borel and satisfy uniform Lipschitz and the growth conditions. Consequently, there exists a separable, measurable and almost surely sample continuous process which is the unique solution of the Itô stochastic differential equation (37).

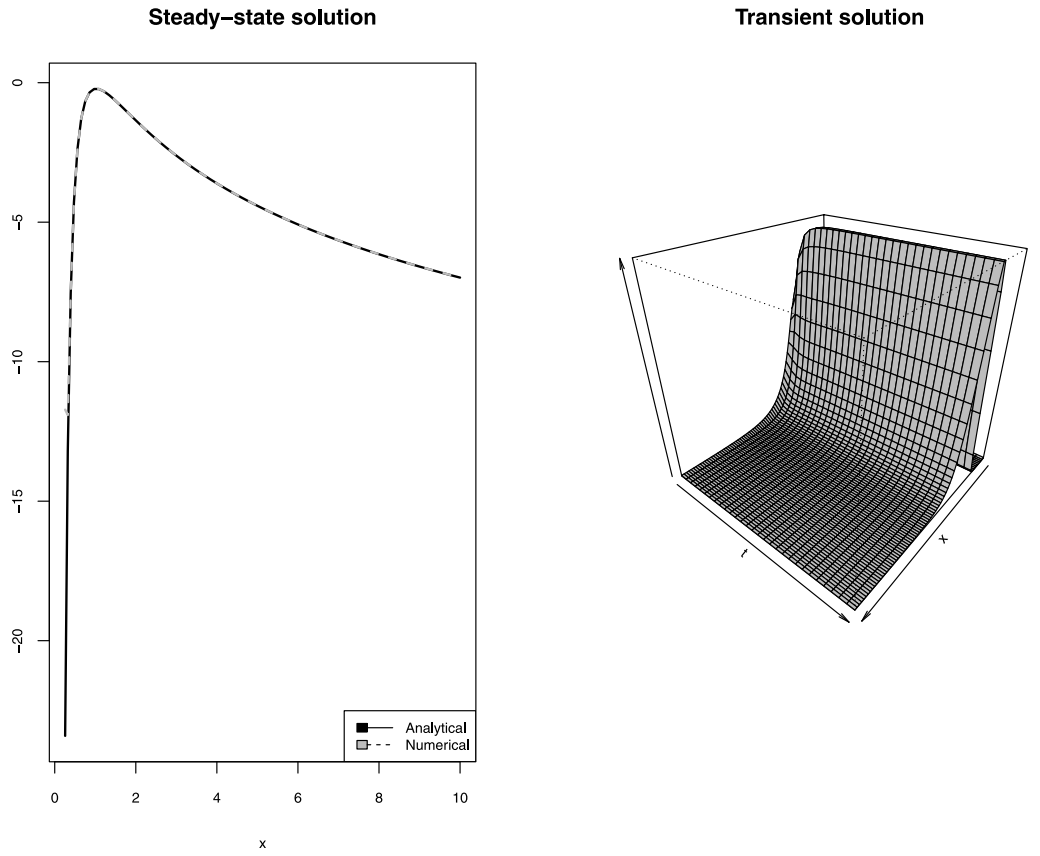

Fig. 4. Cubic diffusion with $A = 0.1$, $B = 2$, $C = 1$. (a) Comparison of the numerical and analytical steady-state solutions in log scale. (b) Transient numerical solution. $E_{rel} = 0.003$.

The stationary ergodic distribution is of the form:

$$cub(x) = \frac{2\left(\frac{B}{C^2}\right)^{\alpha+1} x^{-2\alpha-3}\exp(-\frac{B}{C^2x^2})}{\Gamma(\alpha+1)},\ x>0, B>0,\ C>0, \alpha+1>0, \tag{38}$$

where $\alpha = \frac{1}{2} - \frac{A}{C^2}$. The corresponding Fokker–Planck equation is of the form:

$$\frac{\partial}{\partial t}p(x,t) = -\frac{\partial}{\partial x}[(Ax^3+Bx)p(x,t)] + \frac{1}{2}\frac{\partial^2}{\partial x^2}[C^2x^4p(x,t)], \quad x\in\mathbb{R}, t\geq 0.$$

Fig. 4(a) presents the numerical approximation of the cubic diffusion on log scale when it converges to the steady-state solution with parameters $A = 0.1$, $B = 2$, $C = 1$. For the reduced basis approximation we use two basis function and $\alpha_0 = 0.221314$ and $\alpha_1 = 2.5447711 \times 10^{-14}$. Fig. 4(b) presents transient numerical solution with the same parameters.

4.4. F-diffusion

The F-distribution is an asymmetric distribution and it arises frequently as the null distribution of a test statistic, most notably in the analysis of variance. Consider the following SDE, where the state space is $0 \leq l < r \leq \infty$,

$$dX(t) = -\theta\left(X(t) - \frac{\beta}{\beta-2}\right)dt + \sqrt{\frac{4\theta}{\alpha(\beta-2)}X(t)(\beta+\alpha X(t))}dW(t), \quad \theta>0,\ t\geq 0,\ \alpha\geqslant 2,\ \beta>2. \tag{39}$$

Then the ergodic distribution has the following form

$$fi(x) = \frac{\alpha^{\alpha/2}\beta^{\beta/2}}{B(\alpha/2,\beta/2)}\frac{x^{(\alpha/2)-1}}{(\beta+\alpha x)^{(\alpha+b)/2}},\ x\geq 0. \tag{40}$$

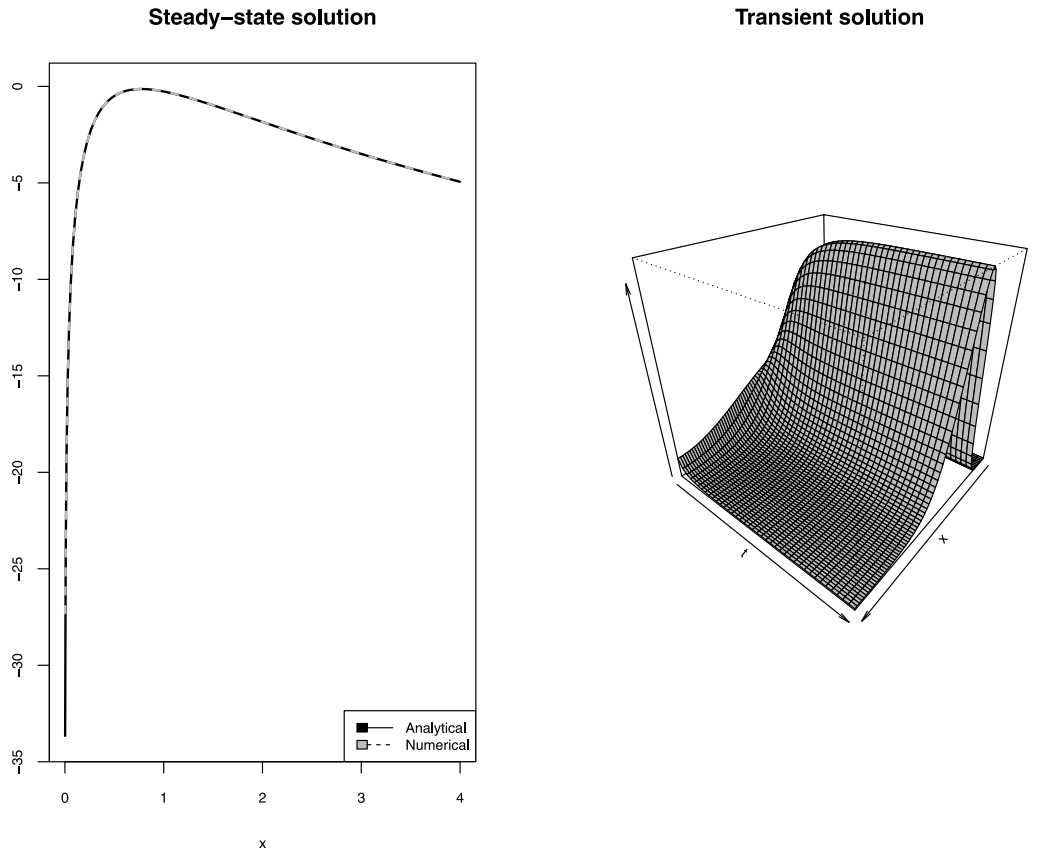

Fig. 5. F-distribution diffusion with $\alpha = 17$, $\beta = 14$. (a) Comparison of the numerical and analytical steady-state solutions in log scale. (b) Transient numerical solution. $E_{rel} = 0.006$.

where $B(\alpha, \beta)$ is the beta function. This is none other than the log F distribution which dates back to Fisher (see Madan et al. [20], for example). The corresponding Fokker–Planck equation is of the form

$$\frac{\partial}{\partial t}p(x,t) = -\frac{\partial}{\partial x}\left[-\theta\left(x - \frac{\beta}{\beta-2}\right)p(x,t)\right] + \frac{1}{2}\frac{\partial^2}{\partial x^2}[(\frac{4\theta}{\alpha(\beta-2)}x(\beta+\alpha x))p(x,t)], \quad x \in \mathbb{R}, t \geq 0.$$

Fig. 5(a) presents the numerical approximation of the F-distribution diffusion in log scale when it converges to the steady-state solution with parameters $\alpha = 17$, $\beta = 14$. For the reduced basis approximation we use two basis function and $\alpha_0 = 0.538483$ and $\alpha_1 = 3.0333233 \times 10^{-15}$. Fig. 5(b) presents transient numerical solution with the same parameters.

5. Discussion

In this paper we considered examples of different types of hyperbolic distributions and their corresponding transient Fokker–Planck equations. Although we know that the stationary distribution of the hyperbolic diffusions processes follow the HD, the transient solution has no closed form expression and therefore we need to resort to numerical methods to obtain the time-dependent behaviour of these diffusions.

Despite the fact that applications of hyperbolic distribution processes can be found in many areas of science including, for example, financial data, environmental modelling, and wind turbulence, there are relatively few research papers in this area due to the complexity of the model. In this paper we have presented an efficient numerical approximation for modelling the behaviour of transient hyperbolic diffusion processes. The approximation is based on spectral methods which are high-order discretization methods that use global basis functions which interpolate the solution at the Gauss–Lobatto Legendre nodes. Spectral methods are used since they possess practical advantages over other discretization methods, such as the ability to obtain the prescribed level of accuracy with a significantly reduced number of degrees of freedom.

Spectral approximations have been used in conjunction with an adaptive reduced basis method which has been shown to be effective and efficient for solving the high-dimensional Fokker–Planck equations that arise in many areas of science

and engineering. This technique has been applied in this paper to obtain accurate and efficient approximations to the transient behaviour of hyperbolic diffusions.

Very few degrees of freedom are required to achieve extremely accurate approximations. This evidenced in the numerical results section where it is shown that only two basis functions are required in conjunction with a spectral approximation using $N = 80$. This suggests that other types of hyperbolic diffusions can be solved in a similar manner. In this paper we have only considered cases where the corresponding Fokker–Planck equation is known. Other more complicated cases and where the diffusion term has a complicated form are open areas for future research.

Data availability

Data will be made available on request.

References

[1] T.H. Rydberg, Generalized hyperbolic diffusion processes with application in finance, Math. Finance 9 (2) (1999) 183–201.
[2] B.M. Bibby, M. Sørensen, A hyperbolic diffusion model for stock prices, Finance Stoch. 1 (1) (1997) 24–41.
[3] R. Gutierrez, R. Gutierrez-Sanchez, A. Nafidi, E. Ramos, A diffusion model with cubic drift: Statistical and computational aspects and application to modelling of the global CO2 emission in Spain, Environmetrics 18 (2007) 55–69.
[4] Y.K. Tse, X. Zhang, J. Yu, Estimation of hyperbolic diffusion using the Markov chain Monte Carlo method, Quant. Finance 4 (2004) 158–169.
[5] O.E. Barndorff-Nielsen, Exponentially decreasing distributions for the logarithm of particle size, Proc. Royal Soc. Lond. Ser. A 353 (1977) 401–409.
[6] O. Barndorff-Nielsen, P. Blaesild, J.L. Jensen, M. Sørensen, The fascination of sand, in: A.C. Atkinson, S.E. Fienberg (Eds.), A Celebration of Statistics, Springer, New-York, 1985, pp. 57–87.
[7] G.M. Leonenko, T.N. Phillips, On the solution of the Fokker–Planck equation using a high-order reduced basis approximation, Comput. Methods Appl. Mech. Engrg. 199 (1–4) (2009) 158–168.
[8] G.M. Leonenko, T.N. Phillips, High-order approximation of Pearson diffusion processes, J. Comput. Appl. Math. 236 (11) (2012) 2853–2868.
[9] G.M. Leonenko, T.N Phillips, Numerical approximation of high-dimensional Fokker–Planck equations with polynomial coefficients, J. Comput. Appl. Math 273 (2015) 296–312.
[10] C. Canuto, M.Y. Hussaini, T.A. Zang Jr., A. Quarteroni, Spectral Methods in Fluid Dynamics, second ed., Springer, Heidelberg, 1991.
[11] F. Chinesta, A. Ammar, E. Cueto, Recent advances and new challenges in the use of the proper generalized decomposition for solving multidimensional problems, Arch. Comput. Methods Eng. 17 (4) (2010) 327–350.
[12] P. Chinesta, E. Cueto, A short review in model order reduction based on proper generalized decomposition, Arch. Comput. Methods Eng. 18 (2011) 395–404.
[13] C. Ghnatios, G. Xu, A. Leygue, M. Visonneau, F. Chinesta, A. Cimitiere, On the space separated representation when addreng the solution of PDE in complex domains, Disc. Cont. Dyn. Syst. 9 (2016) 475–500.
[14] C. Ghnatios, E. Abisset, A. Ammar, E. Cueto, J.-L. Duval, F. Chinesta, Advanced separated spatial representations for hardly separable domains, Comput. Meth. Appl. Mech. Engng. 354 (2019) 802–819.
[15] R. Chinesta, A. Leygue, The Proper Generalized Decomposition for Advanced Numerical Simulations, Springer, Heidelberg, 2014.
[16] B.M. Bibby, I.M. Skovgaard, M. Sørensen, Diffusion-type models with given marginal distribution and autocorrelation function, Bernoulli 11 (2) (2005) 191–220.
[17] A. Ammar, D. Ryckelynck, F. Chinesta, R. Keunings, On the reduction of kinetic theory models related to finitely extensible dumbbells, J. Non-Newton. Fluid Mech. 134 (2006) 136–147.
[18] K. Pearson, Tables for Statisticians and Biometricians, Cambridge University Press, Cambridge, 1914.
[19] D.B. Madan, P.P. Carr, E.C. Chang, The variance gamma process in option pricing, Eur. Financ. Rev. 2 (1998) 79–105.
[20] M.M. Meerschaert, A. Sikorskii, Stochastic Models for Fractional Calculus, De Gruyter, Berlin/Boston, 2019.